

Received December 30, 2020; reviewed; accepted April 13, 2021

A study on the dissolution kinetics of iron oxide leaching from clays by oxalic acid

Volkan Arslan

General Directorate of Minerals Research and Exploration, 42100, Konya, Turkey.

Corresponding author: volkanarslan76@hotmail.com

Abstract: Clay is widely used in a number of industries due to its special properties like fine particle size, brightness and whiteness, chemical inertness, platy structure, etc. In this study, the general characteristics of clays have been investigated by XRF, XRD, FT-IR, TG-DTA and SEM. The presence of iron as an impurity decreases its commercial value due to giving unwanted colors to clay mineral. Therefore, the dissolution capacity of clay ore was investigated by oxalic acid leaching. Under optimized leaching conditions (0.8 M oxalic acid concentration, 85°C reaction temperature, 1.75 ambient pH, -106+75 µm particle size, 15% w/v solids concentration and 150 min. leaching time) with 250 rpm stirring, 83.90% of Fe₂O₃ was removed. The amount of iron oxide, the main impurity in the clay, has been reduced from 2.70 to 0.40%. The iron dissolution kinetics was mainly controlled by internal diffusion control of shrinking core model and activation energy, E_a, of 26.29 kJ/mol was obtained for the process. The results also showed that the studied clays have adequate characteristics for ceramics industry, earthenware and porcelain production.

Keywords: clay, physico-chemical characterization, chemical leaching, oxalic acid, dissolution kinetic, activation energy

1. Introduction

Clay is a term used to describe either the size of the individual particles present in a deposit (clay size fraction) or specific minerals (clay minerals) of small size typically less than 0.002 mm in dimension. This mineral mostly contains impurities such as limestone, silica, mica, and iron oxide and has a yellowish, reddish, or brown color (Fabio et al., 2009; Vitra, 2009; Nzeukou et al., 2013; Abuh et al., 2014; Njoka et al., 2015). The chemical and physical properties of clay minerals are of great importance to industry, agriculture and the environment owing to their abundance, high specific surface area, high layer charge, laminar morphology and chemical reactivity with both neutral and charge species (Murray, 1999; Hoidy et al., 2009). Clays are used as raw materials in many industrial fields such as ceramics, paper, paint, petroleum industry, clarification of various effluents, catalysis, pharmaceutical, cosmetics and tooth paste industries. The common impurities of the natural mineral are iron oxides and quartz, which impart poor quality to the finished products and cause other problems, if present in excess. For the production of high-quality materials, the iron content in clay should be lower than 0.8% (Celik, 2010). Many methods, such as flotation, gravity separation, chemical leaching, reductive roasting and magnetic separation are used for the beneficiation of clay (Chang, 2002; Abel, 2012; Fadil-Djenaboua, 2015; Milosevic, 2017).

Chemical leaching is a method that aims to remove unwanted contaminants from minerals using organic and inorganic acids. Among the inorganic acids, the most widely used are hydrofluoric, hydrochloric, sulfuric and perchloric acids. Especially HF, are very dangerous to human health and the environment, and must be recycled. On the other hand, the clay products must be required washing after the leaching, since hydrochloric and sulfuric acids can easily contaminate the product with SO₄²⁻ and Cl⁻ (Santos et al., 2015; Tuncuk and Akcil, 2016). Organic acids (oxalic, citric, ascorbic, gluconic,

malic acid) are often preferred because of their advantages such as higher iron removal yield, ability to proceed in a wide pH ranges as they prevent iron precipitation and being a more eco-friendly product compared to inorganic acids (Paniyas et al., 1996; Mandal and Banerjee, 2004; Lee et al., 2006; Lori et al., 2007; Zhong et al., 2013; Tuncuk and Akcil, 2016; Lima et al., 2017; Vapur et al., 2017; Garg and Skibsted, 2019; Pariyan et al., 2019). Especially, oxalic acid has been reported to be more effective for iron removal and brightness improvement (Ambikadevi and Lalithambika, 2000).

Leaching kinetics is important in dissolving metals and metal compounds and in designing the leaching process. To optimize the leaching efficiency, the dissolution kinetics should be very well analyzed. The major models that have been developed for non-catalytic fluid-solid reactions are the shrinking core, shrinking particle, homogeneous, grain, uniform pore and random pore models (Gbor and Jia, 2004; Ghassa et al., 2017). Among these models, the shrinking core model has been widely used in the area of hydrometallurgy to model leaching systems. A model is determined according to the results of the leaching experiments and the data obtained from the model are used to determine the activation energy (Cornell and Schwertmann, 2003; Bonneville et al., 2009; Hursit et al., 2009; Shi et al., 2011; Sultana et al., 2014; Ghasemi and Azizi, 2017; Lima et al., 2017; Zhang et al., 2017; Li et al., 2019; Yang and Li, 2020).

In this study, X-ray fluorescence spectroscopy (XRF), X-ray diffraction (XRD), scanning electron microscope (SEM), thermo gravimetric-differential thermal analysis (TG-DTA) and fourier transformed infrared spectroscopy analysis (FT-IR) were performed to determine the characteristic properties of clay. After that, organic acids such as citric, oxalic, malic, gluconic, malonic acid were used to select the most suitable acid for this study in the first stage chemical leaching experiments and the most suitable organic acid was determined. In the second stage leaching experiments, the clay sample was subjected to chemical leaching with oxalic acid ($C_2H_2O_4$) to make it suitable for various industries such as filling, coating, ceramic, paint, cement etc. In the research on dissolution kinetics, dissolution curves were drawn, activation energy was calculated and it was investigated whether it was suitable for chemical leaching reaction using oxalic acid.

2. Materials and methods

2.1. Material

Iron-containing clay from Doganhisar region in Turkey was selected for experimental studies. The study covered over approximately 25 km² including Ayaslar and Doganhisar formations. The clay sample was passed through a 500 µm diameter sieve before use. The sample was used as such without any further modification for the acid leaching treatments.

2.2. Characterization techniques

The clay sample was characterized by XRF, XRD, FT-IR, TG-DTA and SEM. All characterization analyzes were performed in General Directorate of Mineral Research and Exploration Analysis Laboratory and Hitit University Scientific Research Center. The chemical composition was determined by X-ray fluorescence spectroscopy (PW2400, Phillips) with X-ray tube of rhodium anode and scintillation detector with a current 40 mA and voltage 40 mV. Bulk clay samples crushed to fine powder were mixed lithium tetra borate for chemical analysis. The ignition loss was measured by calcination at 1000°C. The X-ray diffraction data was collected using a Philips analytical X-ray instrument, X'Pert-MPD (PW 3020 vertical goniometer and PW 3710 MPD control unit) employing Bragg-Brentano para focusing optics. The XRD patterns were recorded in the range of 10-70° with a scanning rate of 2°/min. Morphology of the clay samples was determined by SEM. The samples were deposited on a sample holder with an adhesive carbon foil and sputtered with gold. The clay samples were studied with a Philips 30 Analytical Scanning Electron Microscope. Particle images were obtained with a secondary electron detector. Simultaneous thermal analysis (Netzsch STA 409) under air atmosphere was used for differential thermal analysis and thermo-gravimetric analysis (DTA/TGA). The temperature was increased from room temperature to 1200°C at a rate of 10°C/min, kept at this maximum temperature for 10 min. FT-IR spectra were recorded on a Perkin-Elmer infrared

spectrophotometer as KBr pellets with resolution of 4 cm^{-1} , in the range of $450\text{--}4000\text{ cm}^{-1}$. The sample and analytical grade KBr were dried at 100°C over-night prior to the FT-IR analysis.

2.3. Chemical leaching experiments

In the first stage chemical leaching experiments, the efficiency of various organic acids was investigated. For all experiments very pure (>99%) citric (Merk), oxalic (Merk), malic (Merk), gluconic (Merk) and malonic (Merk) acids were used as reducing agents. Chemical leaching experiments performed to determine the most suitable organic acid in 500 ml flasks, 400 ml acid solution, 250 rpm stirring speed, 0.5 M acid concentration, 60°C leaching temperature, 2.00 ambient pH, $-106+75\ \mu\text{m}$ particle size, 15% solid concentration and 120 minutes leaching time. In the first stage experiments, the most effective organic acid was determined and the effect of this acid on Fe_2O_3 and TiO_2 removal from the clay was investigated under varied leaching conditions.

In the second stage chemical leaching experiments, the leaching tests were carried out in a round bottomed flask (500 ml) which was kept stirred in a heating mantle, for each run, 400 ml of oxalic acid solution ($\text{C}_2\text{H}_2\text{O}_4$, reagent grade) at different concentrations were added to the flask and the temperature was set to the desired value. Then, 40.0 g of clay was added to the flask while 250 rpm magnetic stirring. Periodically, a 10 ml sample was taken from the leach slurry and was centrifuged immediately at 250 rpm during 20 min. A clear 5 ml aliquot of the solution was collected for total iron determination. All leaching tests were made at atmospheric pressure. A watch glass was fitted to the flask to prevent evaporation. Subsequently, the slurry was filtered, and the residue was washed with hot distilled water, dried, and analyzed for iron using atomic absorption spectrophotometer (AAS). Experiments were done in triplicate. The variables studied were oxalic acid concentrations (0.01, 0.05, 0.10, 0.30, 0.50, 0.80 and 1.0 M), reaction temperature (15, 30, 45, 60, 75, 85 and 100°C), pH (1.25, 1.50, 1.75, 2.00, 2.25, 2.50 and 3.00), particle size ($-500+250$, $-250+150$, $-150+106$, $-106+75$ and $-75+38\ \mu\text{m}$), solids concentration (5, 10, 15, 20, 25, 30 and 40 w/v) and leaching time (30, 60, 90, 120, 150, 180 and 210 min). The clay leaching process was simulated using the SuperPro Designer Program and the flow sheet of the experimental steps was given in Fig. 1.

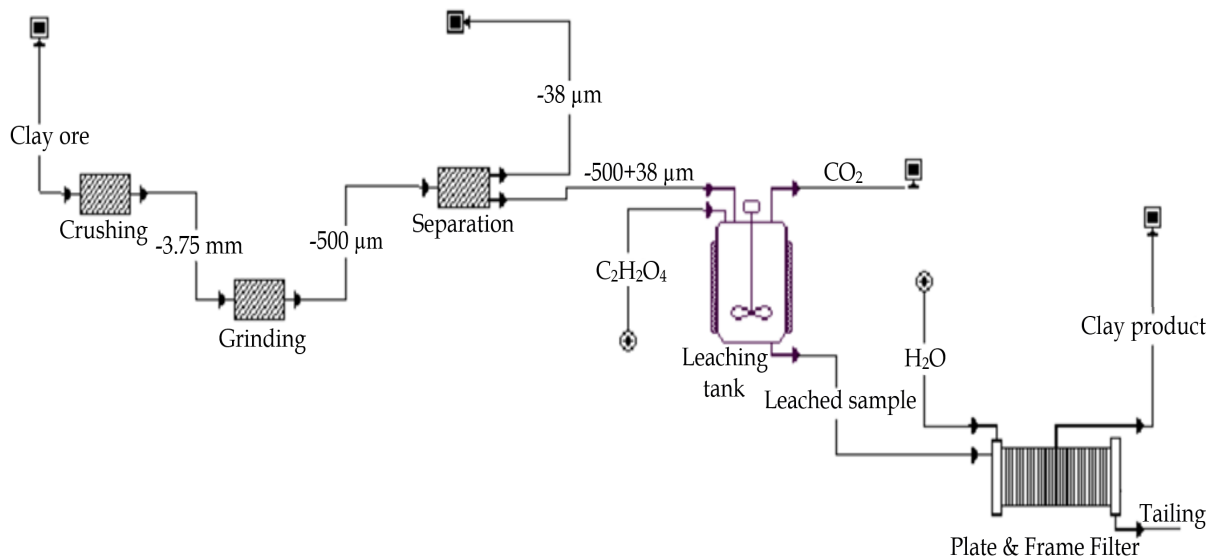


Fig. 1. Clay product flow sheet created with SuperPro Designer Software

2.4. Kinetic study of leaching process

In a heterogeneous solid/liquid leaching reaction system, the soluble reactants diffuse across the interface and/or through the solid layer first (Zhang et al., 2016; Li et al., 2017; Tao et al., 2021). The shrinking core model assumes that the solid particles used in the experiments gradually shrink during the leaching process, leading to the formation of a porous layer on the surface of the unreacted core. The shrinking core model is one of the most important and widely used kinetic models in leaching of

clay minerals. Experimental data graphic is plotted against time of each model equation to determine the controlling step. The model with the closest correlation coefficient to one is thought to best control the leaching process (Dehgan et al., 2009; Sultana and Kurny, 2012; Legorreta et al., 2015; MacCarthy et al., 2016; Tanda et al., 2018; Pariyan et al., 2019; Cetintas and Bingol, 2020).

If the reaction rate is controlled by a surface chemical reaction, the integrated rate equation of the shrinking core model can be described as follows:

$$1 - (1 - \alpha)^{1/3} = k_r t \quad (1)$$

If the reaction rate is controlled by diffusion through the product layer, the integrated rate equation of the shrinking core model can be described as follows:

$$1 - 2/3\alpha - (1 - \alpha)^{2/3} = k_d t \quad (2)$$

where α is the fraction of the clay ore reacted, t is the leaching time (min), k_r is the apparent rate constant for the surface chemical reaction, k_d is the apparent rate constant for the diffusion through the product layer (Antonijevic et al., 2004; Baba and Adekola, 2012; Baba et al., 2014; Baba et al., 2015; Zhang et al., 2019).

The Arrhenius equation is a formula for the temperature dependence of reaction rate. This equation has a vast and important application in determining rate of chemical reactions, and for calculation of activation energy, as well. The activation energy for mentioned reactions could be calculated by Arrhenius equation (Eq. 3):

$$\ln(k) = \ln(A) - \frac{E_a}{R} \cdot \frac{1}{T} \quad (3)$$

where, A is a pre-exponential factor (mol/cm²-s), E_a is the apparent activation energy (kJ/mol), and R is the molar gas constant (kJ/mol-K) (Ayanda and Adekola, 2012; Du et al., 2016; Sanda and Taiwo, 2016; Naviaux et al., 2019).

3. Results and discussion

3.1. Chemical and mineralogical compositions

From the phase (mineralogical) analysis and XRD report it could be concluded that the major component of the clay is mica and illite, followed by quartz, calcite, feldspar and trace amounts of chlorite in decreasing order of abundance (Fig. 2). The chemical composition of the sample was given in Table 1. Size distribution of the sample was as follows: -500+250 μm : 14.27%, -250+150 μm : 20.13%, -150+106 μm : 30.32%, -106+75 μm : 31.83%, -75+38 μm : 3.45%.

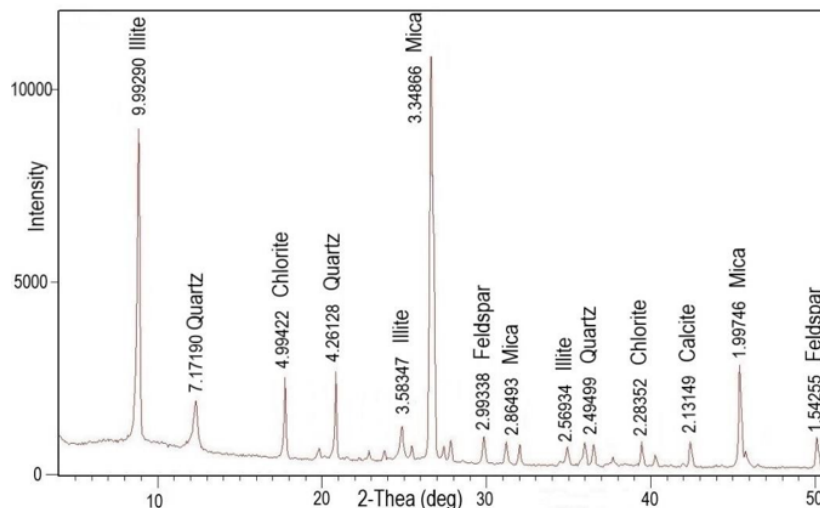


Fig. 2. X-ray diffraction patterns for a Doganhisar clay sample

Table 1. The chemical composition of the clay sample

Composition	SiO ₂	Al ₂ O ₃	Fe ₂ O ₃	MgO	CaO	P ₂ O ₅	K ₂ O	TiO ₂	LOI	Whiteness
Content (wt, %)	62.40	20.63	2.70	0.60	0.25	0.30	2.56	1.04	7.21	61.06

3.2. Thermal analysis (DTA/TGA)

In general, clay materials contain three kinds of water molecules in their structure. First layer, the physisorbed and interlayer water are loosely bound and are mobile that they can be removed by heat treatment below 200°C. The water molecules present in the first coordination sphere of the interlayer ions is strongly bonded and require higher temperature in the range of 250-450°C for their removal. Finally, the structural hydroxyl groups can condense and dehydrate in the temperature range of 450-750°C. DTA can be applied to identify and to estimate various types of clay minerals. These minerals can be differentiated by determining the temperature at which the endothermic and exothermic peaks occur. From the TG analysis, it was found that the clay sample lost all its moisture till 100-150°C. Since the total weight loss in the clay mineral is not much at high temperatures, this indicates that it can be used at high temperature applications. Besides, DTA curve gave an exothermic peak at 450-470°C and this endothermic peak supported that thermal degradation took place between 450 and 700°C. The reaction decomposition started at 610°C, made an endothermic peak at about 730°C, and was complete at 925°C (Fig. 3). In the review of the literature, it was determined that the clay in this region shows similar properties (Rahman and Muneer, 2005; Wu et al., 2011; Sandler, 2013; Celik et al., 2013; Erdogan, 2015). As a complementary remark regarding the thermal analysis, it should be mentioned that the common characteristics for all clays are the presence of two ranges of endothermic peaks, which are related to the decomposition of Al and Fe hydroxides and the dehydroxylation of the clay mineral.

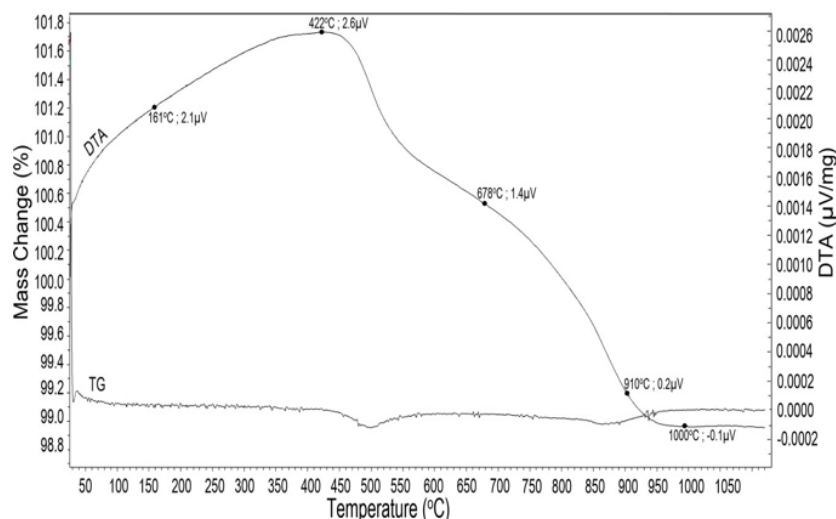


Fig. 3. TG-DTA curves of Doganhisar clay (heating rate: 10°C/min)

3.3. Fourier transformed infrared (FT-IR) analysis

Fig. 4 shows the FT-IR spectra of the clay sample. They range from 550 to 3000 cm^{-1} . The peaks at position 570.05, 695.78, 751.15, 801.43, 911.68 and 1000.94 cm^{-1} lies within the mid infrared region (550-1000 cm^{-1}). The spectrum of the original clay suggests that it contains poorly crystallized components, evidenced by the absorption band at 1000 cm^{-1} and inflexion at 1220 cm^{-1} due to amorphous silica. The raw clay spectrum also contains a broad band at 1450 cm^{-1} , due to the calcite impurity. The IR spectra also suggest that the Al^{3+} , Fe^{3+} and Mg^{2+} ions occupy octahedral sites, since the hydroxyl bending peaks of Al_2OH , AlFeOH and AlMgOH vibrations are present at 911.68 and 801.43 cm^{-1} respectively. An O-H stretching band located around 2351 cm^{-1} has been reported in Mg and Al-enriched dioctahedral mica (Madejova et al., 1998; Gates et al., 2002; Temuujin et al., 2002; Temuujin et al., 2004; Njoka et al., 2015).

3.4. Scanning electron microscopy (SEM)

Representative scanning electron micrographs of the clay sample is presented in Fig. 5 which shows the morphological features. On further examination of SEM micrographs, the larger clay mineral

particles seems to consist of much smaller platelets which indicates that the clay sample is made up of very fine particles. It shows a sample composed entirely of well-rounded quartz with small oval depression fringed by clay. The presence of iron oxide has been shown by appearance of very bright sections and this confirms the results of XRD and FT-IR.

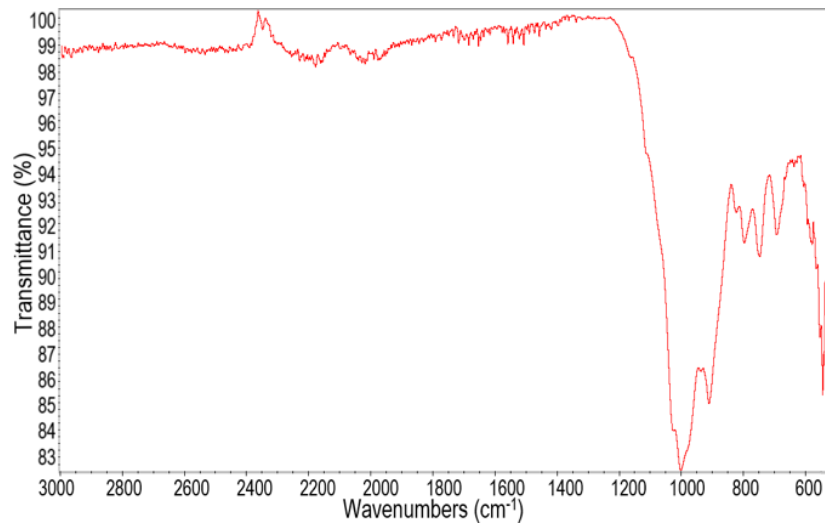


Fig. 4. FT-IR spectrum of clay sample from Doganhisar formation

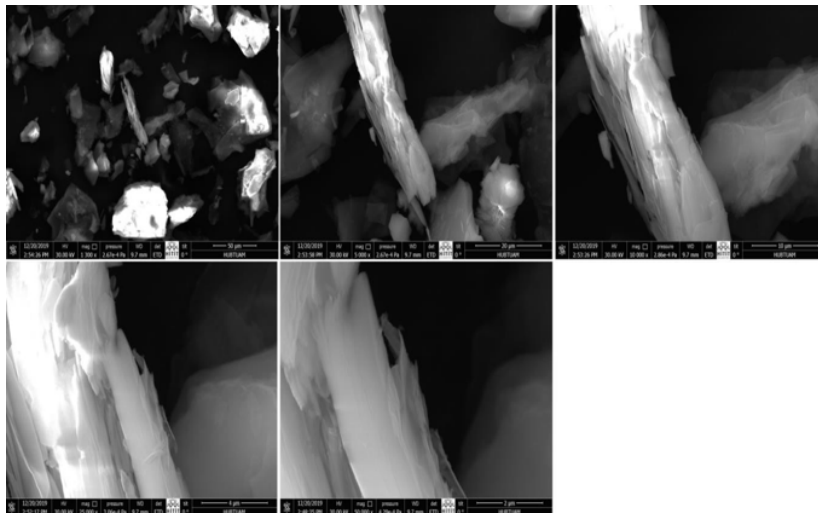


Fig. 5. SEM photomicrographs of clay sample from Doganhisar formation

3.5. Chemical leaching results

3.5.1. Determination of the optimized organic acid

The effects of different organic acids on the ability to dissolve Fe_2O_3 and TiO_2 in clay are shown in Table 2. Oxalic acid has been found to be the most effective leachant. Also, the order of activity of organic acids is as follows: oxalic>citric>malonic>gluconic>malic acid. Achieving the best results with oxalic acid can be explained by its acidity, reducing capacity, and complexing effect (Ambikadevi and Lalithambika, 2000; Saikia et al., 2003).

3.5.1. Oxalic acid leaching results

3.5.1.1. Effect of pH on the iron dissolution efficiency

In this experiment, the effect of pH on iron dissolution efficiency was investigated. Chemical leaching experiments with pH varied from 1.00 to 3.00 were carried out versus time at 50°C , at 0.3 M oxalic acid concentration, $-150 + 106 \mu\text{m}$ particle size and 20% solids rate. It was observed that above pH 2.0, the

amount of dissolved iron in the filtered solution rapidly decreased. This is probably because iron starts to precipitate when pH is greater than 2 (Fig. 6). Investigating the effect of pH, very high iron dissolution efficiency could not be obtained and the best dissolution efficiency was found as 28.75% at pH 1.75.

Table 2. Fe₂O₃ content in the clay after chemical leaching with different organic acids

Organic acids	Fe ₂ O ₃ content (%)	TiO ₂ content (%)
Raw material	2.70	1.04
Citric acid	0.93	0.71
Gluconic acid	1.51	0.81
Malic acid	1.78	0.89
Malonic acid	1.23	0.76
Oxalic acid	0.71	0.64

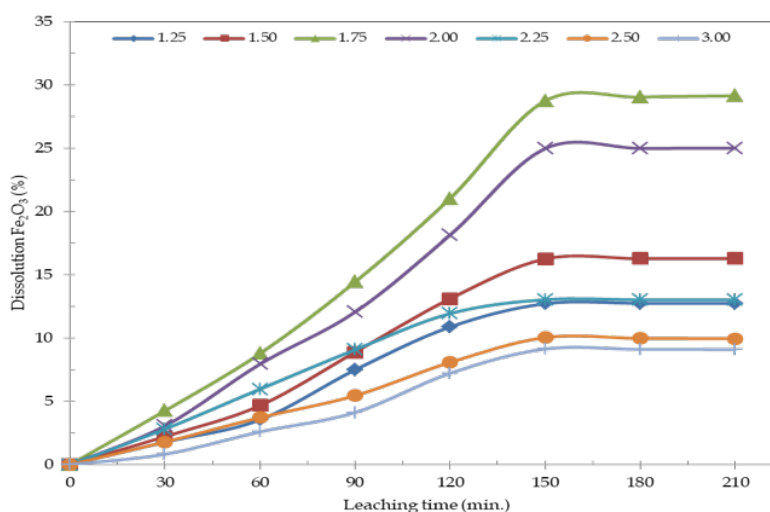


Fig. 6. Effect of pH on iron removal from clay

3.5.1.2. Effect of particle size

The experiments were carried out at pH 1.75, at 50°C, at 0.3 M acid concentration and 20% solids rate. The results of this investigation are summarized in Fig. 7. When Fig. 7 was investigated, it was clearly seen that the dissolution efficiency of the clay ore decreases as the particle size increases. Apparently, the greater the particle size, the lesser the fraction, that is being dissolved owing to the increasing surface area, exhibited by small powdered particle size (Baba et al., 2009). As a result, it was determined that the best iron dissolution efficiency was realized at -106+75 μm particle size in this experiment. In this particle size, iron dissolution efficiency was 36.87%.

3.5.1.3. Effect of solid density

This experiment was carried out by varying the solids ratio from 5 to 40% (w/v) under the optimized conditions of the previous experiment. It was determined that as the solids rate increased, the iron dissolution efficiency increased and then declining slowly after reaching a maximum of 15% (Fig. 8). At higher concentrations (>15%, w/v), the suspension probably becomes sufficiently thick restricting free mixing of clay particles with the leaching solution that results in decrease of the rate (Mandal and Banerjee, 2004). Finally, the optimized solids rate (15% w/v) iron dissolution efficiency was determined as 57.60%.

3.5.1.4. Effect of oxalic acid concentration

The dissolution of iron oxides versus time at 50°C, using various concentrations of oxalic acid (0.01, 0.05, 0.10, 0.30, 0.50, 0.80 and 1.0 M), is shown in Fig. 9. The results depicted in Fig. 9 show that the

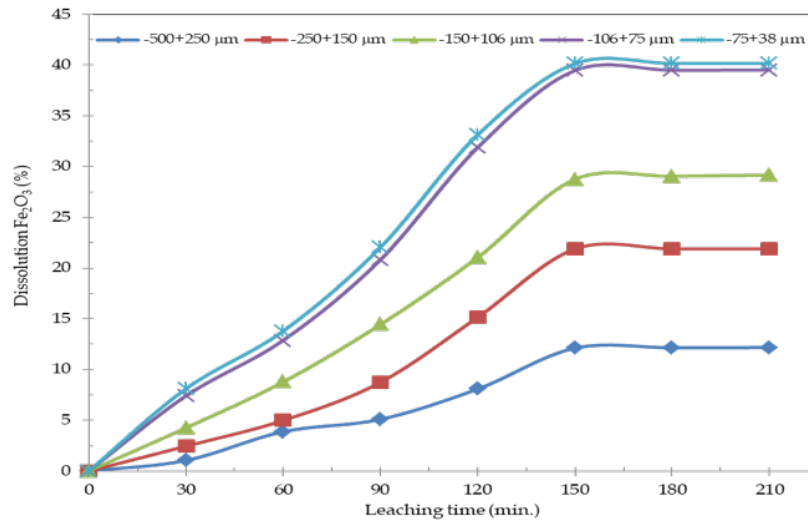


Fig. 7. Effect of particle size on iron removal from clay

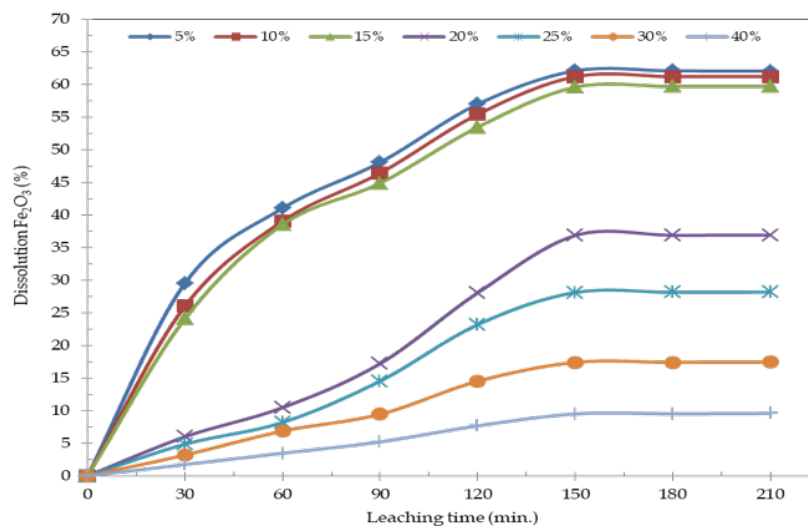


Fig. 8. Effect of solid density on iron removal from clay

yield of the reacted ore increases linearly with increasing acid concentration in the range 0 to 210 min. An increase in the amount of the ore reacted with leaching time were observed within the acid concentration ranges (0.01-0.8 M), where the dissolution increased from 9.50 to 72.60% at 150 min, respectively. However, further increase of the acid to 1.0 M, reduces the amount of the ore reacted to 69.11% at 150 min contact. The possible reason for this observation could be attributed to a precipitation phenomenon (Baba and Adekola, 2012; Baba et al., 2015). Hence, 0.8 M oxalic acid concentration with high value of dissolution was selected for further investigations in this study.

3.5.1.5. Effect of leaching temperature

Oxalic acid concentration was kept constant at 0.8 M and yield of iron dissolution at various temperatures (15, 30, 45, 60, 75, 85 and 100°C) was given in Fig. 10. It was seen that the iron dissolution yield was better especially at temperatures above 75°C. The dissolution curves appear to be parabolic as temperature increases from 45 to 100°C. That is, the dissolution of iron with oxalic acid has to be thermally activated to be efficient. This, on the other hand, is an indicator that the system exhibits a chemical control. The possible reason, as earlier observed, could be due to the retardation of the rate of clay oxidation at elevated temperatures. Hence, the higher the temperature, the higher is the percentage of iron impurities removal (Antonišević et al., 2004; Hernandez et al., 2013; Saklar and Yorukoglu, 2015). At 85°C, for example, the dissolution reached 83.90% within 150 min.

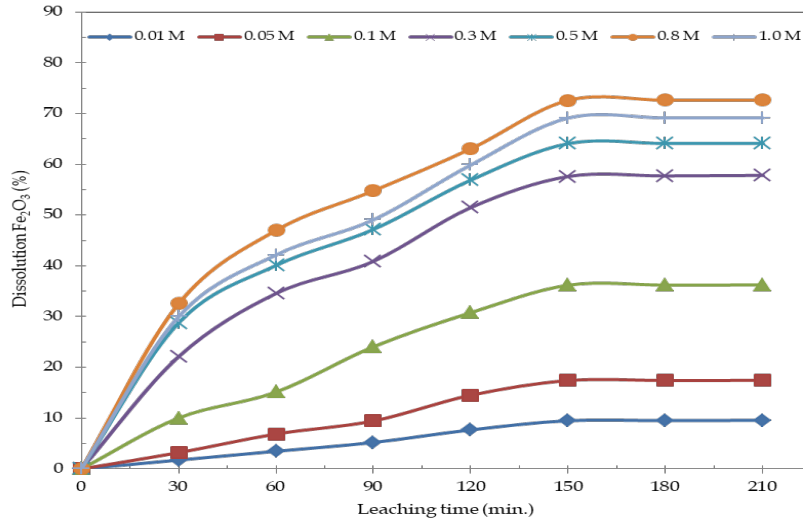


Fig. 9. Effect of oxalic acid concentrations on iron removal from clay

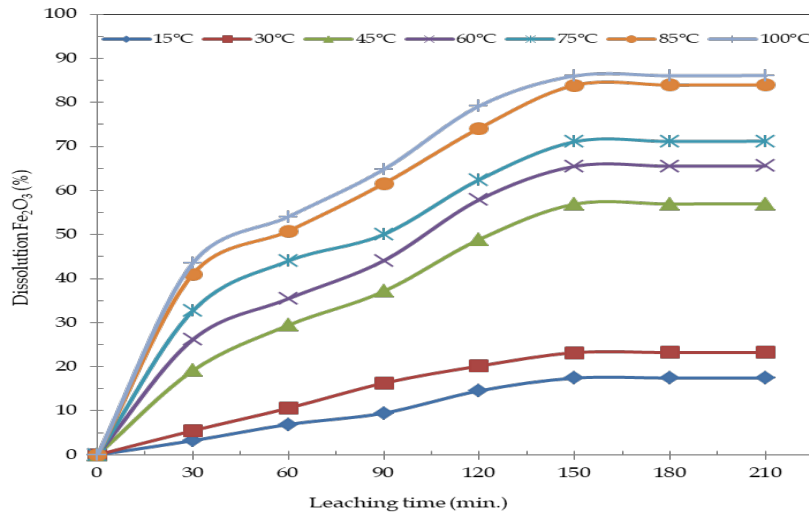


Fig. 10. Effect of leaching temperatures on iron removal from clay

3.6. Dissolution Kinetics Analysis

The results obtained during kinetics study of iron extraction, evaluating the effect of oxalic acid concentration and temperature in the range 298 to 373 K were treated with the decreasing core model for heterogeneous reactions both for diffusive and chemical control. The shrinking core models, which have been tried by several researchers, were tested to explain the dissolution kinetics of the leaching process.

The dissolution data in Figs. 9 and 10 were calculated according to the shrinking core model of Eqs. 1 and 2. It was important to note that the dissolution data fitted perfectly with the model Eq. 1, where an average correlation, R^2 value was obtained. From the leaching time versus $1 - (1 - \alpha)^{1/3}$ plots in Fig. 11, the regression coefficient (R^2) values for the oxalic acid concentrations of 0.01 M, 0.05 M, 0.1 M, 0.3 M, 0.5 M, 0.8 M and 1.0 M were determined as 0.97, 0.98, 0.97, 0.98, 0.93, 0.92 and 0.93, respectively. High R^2 values indicated that the dissolution of iron from the clay mineral was controlled by diffusion. The dissolution data in Fig. 9 were linearized with the model Eq. 1 as seen in Fig. 11.

From Fig. 11, the slope of each lines was calculated and recorded as apparent rate constants, k , from which the plot of $\ln k$, versus $\ln[C_2H_2O_4]$ was obtained (Fig. 12) for the evaluation of reaction order for the process. The plots, shown in Fig. 13, were obtained through Eq. 1 using the dissolution data in Fig. 10. From the graphs drawn for 15, 30, 45, 60, 75, 85 and 100°C temperature values, 0.97, 0.96, 0.97, 0.96, 0.93, 0.89 and 0.89 regression coefficients (R^2) were obtained, respectively. These results indicate that

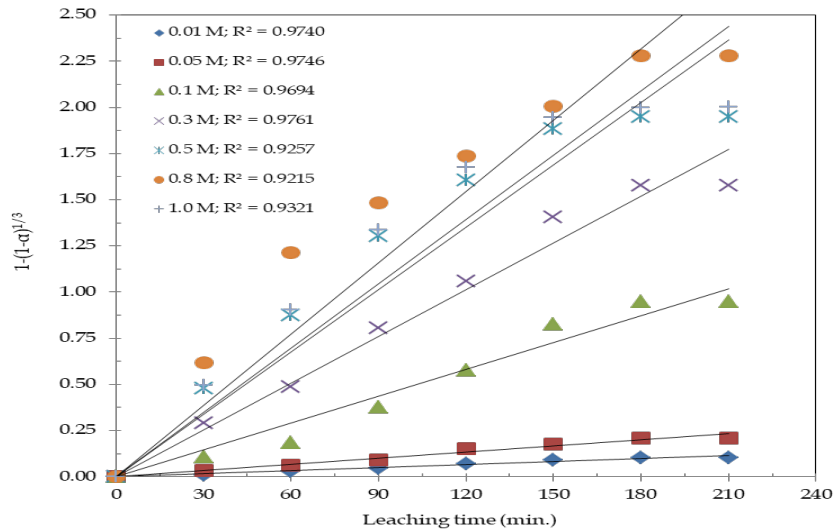


Fig. 11. Plot of $1-(1-\alpha)^{1/3}$ against leaching time at different $[C_2H_2O_4]$

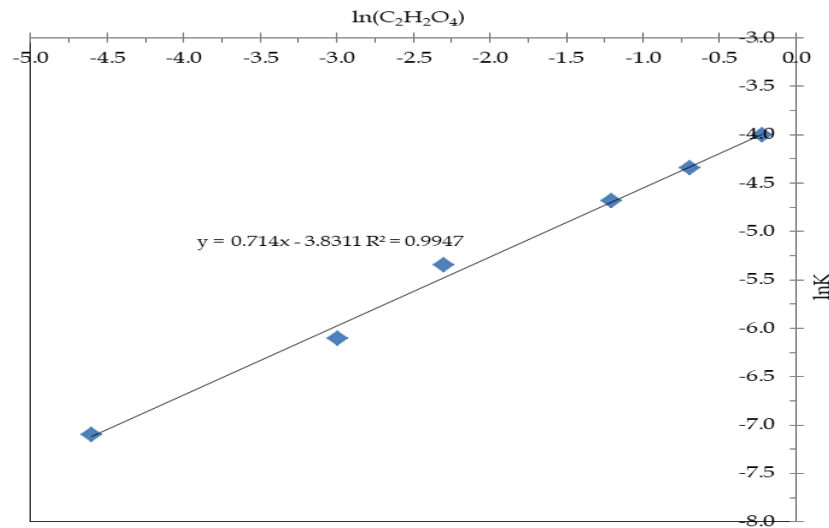


Fig. 12. Plot of $\ln k$ vs. $\ln[C_2H_2O_4]$

iron dissolution from the clay mineral occurs by diffusion through an inert product layer. The Arrhenius plot considering the apparent rate constants, k_r , was obtained by applying Eq. 1 to leaching experimental data (Fig. 14). From the slope of Fig. 14, using Eq. 3, the activation energy (E_a) for the dissolution of clay in $C_2H_2O_4$ is $26.29 \text{ kJ mol}^{-1}$. This value clearly suggests that the reaction for this process is diffusion controlled as proposed by several investigators (Ajemba and Onukwuli, 2012; Sultana et al., 2014; Legorreta et al., 2015; Gao et al., 2019; Pariyan et al., 2019; Yang and Li, 2020). So, it is reasonable that the iron removal is higher at the elevated temperatures.

3.7. Technological Properties

While the whiteness degree of the untreated clay was 61.06%, the whiteness degree of the clay sample was determined as 90.60% after oxalic acid leaching. This value is much higher than 80% as specified for filling, coating and ceramic grade clay. Usage standard values of raw material and leached clay for filling, coating, ceramic, paint and cement industries were given in Table 3 (IS 5396). It was clearly seen that the raw material, especially because of the Fe_2O_3 and TiO_2 values were above the desired standards, was not suitable for ceramic or other purposes. The clay sample obtained after oxalic acid leaching meets all the requirements in order to be used as a raw material or filler material in the all industries except paint industry. Further study on removal of iron from clay is necessary to obtain higher quality clay from the Doganhisar region.

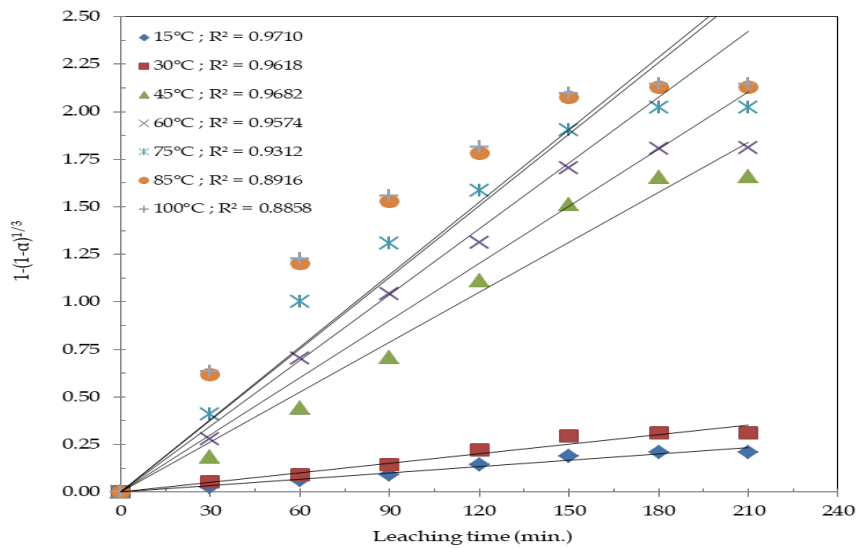
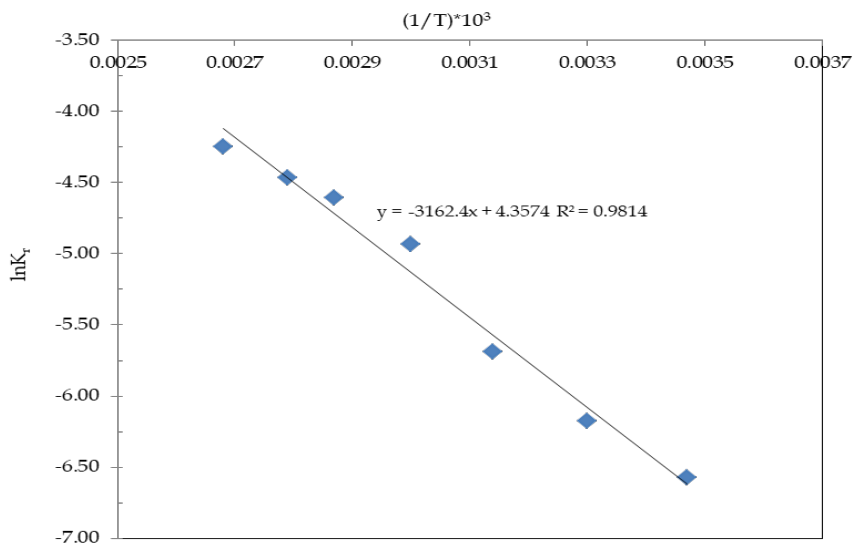
Fig. 13. Plot of $1-(1-\alpha)^{1/3}$ vs. leaching time at different temperaturesFig. 14. Arrhenius relation $\ln k_t$ vs. $1/T$ (1/K)

Table 3. Technical properties of raw material and leached clay and standard values of clay for various industries

Characteristics	Filling ^a	Covering ^a	Ceramic ^a	Paint ^a	Cement ^a	Raw material	Leached clay
Al ₂ O ₃ (min)	20	30	28	39	20	20.63	32.15
SiO ₂ (min)	45	45	59	45	51	62.40	65.60
CaO (max)	1.0	1.0	0.1	0.02	0.1	0.25	0.08
TiO ₂ (max)	0.5	0.5	0.4	0.6	0.5	1.04	0.37
Fe ₂ O ₃ (max)	0.5	0.5	0.5	0.9	0.4	2.70	0.40
K ₂ O (max)	-	-	0.3	0.2	0.5	2.56	0.25
pH of the extract	4.5-7.5	4.5-7.5	4.5-7.5	4.5-7.5	4.5-7.5	-	5.0-5.5
Whiteness (min)	80	80	80	-	-	61.06	90.60
LOI (max)	14.0	15.5	14.0	15.5	14.0	7.21	13.79

^a Turkish Standards Institution TS 5396, 1987

Conclusions

Based on the results obtained in this study, the following conclusions can be drawn:

The Doganhisar clay was characterized by chemical, mineralogical and thermal analysis. All applied methods were in a good agreement. The studied clays have a major content of mica and illite minerals with medium amount of quartz, calcite and feldspar, followed by and trace amounts of chlorite in decreasing order of abundance.

In SEM examinations, it was seen that clay samples are mica minerals. It shows a sample composed entirely of well-rounded quartz with small oval depression fringed by clay. The presence of iron oxide has been shown by appearance of very bright sections.

From the TG analysis, it was found that the clay sample lost all its moisture till 100-150°C. Besides, DTA curve gave an exothermic peak at 450-470°C and this exothermic peak supported that thermal degradation took place between 450 and 700°C. Sintering started at around 400°C and was completed at 700°C.

Chemical methods (specially leaching with organic acids) are effective and useful in dissolving iron impurities from clays. Among these organic acids (oxalic, gluconic, citric, malic, malonic, ascorbic acids, etc.), especially oxalic acid is much more effective than others in removing iron in the clay. In chemical leaching experiments, acid concentration, reaction temperature, pH, particle size, solids concentration and leaching time were investigated. The optimized chemical leaching conditions were determined as 1.75 pH, -106+75 μm particle size, 15% w/v solids concentration, 0.8 M oxalic acid concentration, 85°C temperature and 150 min. leaching time. As a result, the amounts of iron oxide and titanium oxide, the main impurities in the clay, were reduced from 2.70% to 0.40% and from 1.04% to 0.37%, respectively in the optimized leaching conditions.

In the research on dissolution kinetics, dissolution curves were analyzed and determined to be suitable for chemical reaction. As a result of the calculations, the activation energy was determined as 26.29 kJ mol⁻¹. Consequently, Doganhisar clay has qualities necessary for the manufacture of stoneware and porcelain industry, and it is an alternative raw material for the filling, covering, ceramic and cement industries.

Acknowledgments

I am grateful to Tokluoglu Mining Company for the supply of clay samples, General Directorate of Mineral Research and Exploration Analysis Laboratory and Hitit University Scientific Technical Application and Research Center for all analyses.

References

- ABEL, O.T., OLADIMEJI, L.A., OLUWATOYIN, O.A., 2012. *Compositional Features and Industrial Application of Ikere Kaolinite Southwestern Nigeria*. Res. J. Engineer. Appl. Sci. 1, 5, 327-333.
- ABUH, M.A., ABIA-BASSEY, N., UDEINYA, T.C., NWANNEWUIHE, H.U., ABONG, A.A., AKPOMIE, K.G., 2014. *Industrial Potentials of Adiabo Clay in Calabar Municipal of Cross River State South-South Nigeria*. Asia Pac. J. Sci. Technol. 15, 1, 63-75.
- AJEMBA, R.O., ONUKWULI, O.D., 2012. *Kinetic Model for Ukpok Clay Dissolution in Hydrochloric Acid Solution*. J. Emer. Trends Eng. Appl. Sci. 3, 448-454.
- ANTONIJEVIC, M.M., JANKOVIC, Z.D., DIMITRIJEVIC, M.D., 2004. *Kinetics of Chalcopyrite Dissolution by Hydrogen Peroxide in Sulphuric Acid*. Hydrometallurgy. 71, 3, 329-334.
- AMBIKADEVI, V.R., LALITHAMBIKA, M., 2000. *Effect of Organic Acids on Ferric Iron Removal from Iron-Stained Kaolinite*. Appl. Clay Sci. 16, 133-145.
- AYANDA, O.S., ADEKOLA, F.A., 2012. *Leaching of Nigerian Columbite in Hydrochloric Acid: Dissolution Kinetics*. Int. J. Metall. Eng. 1, 3, 35-39.
- BABA, A.A., ADEKOLA, F.A., 2012. *A Study of the Dissolution Kinetics of a Nigerian Galena Ore in Hydrochloric Acid*. J. Saudi Chem. Soc. 16, 4, 377-386.
- BABA, A.A., ADEKOLA, F.A., BALE, R.B., 2009. *Development of a Combined Pyro- and Hydrometallurgical Route to Treat Zinc-Carbon Batteries*. J. Hazard. Mater. 171, 1, 838-844.
- BABA, A.A., MOSOBALAJE, M.A., IBRAHIM, A.S., GIRIGISU, S., ELETTA, A.A., ALUKO, F.I., ADEKOLA, F.A.,

2015. *Bleaching of Nigerian Kaolin by Oxalic Acid Leaching*. J. Chem. Technol. Metall. 50, 5, 623-630.
- BABA, A.A., OLUMODEJI, O.O., ADEKOLA, F.A., LAWAL, M., AREMU, A.S., 2014. *Quantitative Leaching of a Spent Cell Phone Printed Circuit Board by Hydrochloric Acid*. Metall. Mater. Eng. 20, 2, 119-129.
- BONNEVILLE, S., BEHREND, T., VANCAPPELLEN, P., 2009. *Solubility and Dissimilatory Reduction Kinetics of Iron(III) Oxyhydroxides: A Linear Free Energy Relationship*. Geochim. Cosmochim. Ac. 73, 5273-5282.
- CELIK, A.G., KILIC, A.M., CAKAL, G.O., 2013. *Expanded Perlite Aggregate Characterization for use as a Lightweight Construction Raw Material*. Physicochem. Probl. Miner. Process. 49, 2, 689-700.
- CELIK, H., 2010. *Technological Characterization and Industrial Application of Two Turkish Clays for the Ceramic Industry*. Appl. Clay Sci. 50, 245-254.
- CETINTAS, S., BINGOL, D., 2020. *Dissolution Kinetics of Manganese during Nickel Recovery from High Iron Grade Laterite by Acid Leaching Combined Naoh-Assisted Mechanochemical Technology*. Cumhuriyet Sci. J. 41,2, 397-406.
- CHANG, L.L.Y., 2002. *Industrial Mineralogy Materials, Processes and Uses*. New Jersey: Prentice Hall, USA.
- CORNELL, R.M., SCHWERTMANN, U., 2003. *The Iron Oxides: Structure, Properties, Reactions, Occurrence and Uses*, Wiley-VCH Publishers, New York, USA.
- DEHGHAN, R., NOAPARAST, M., KOLAHDOOZAN, M., 2009. *Leaching and Kinetic Modelling of Low-Grade Calcareous Sphalerite in Acidic Ferric Chloride Solution*. Hydrometallurgy. 96, 4, 275-282.
- DU, R.L., WU, K., XU, D.A., CHAO, C.Y., ZHANG, L., DU, X.D., 2016. *A Modified Arrhenius Equation to Predict the Reaction Rate Constant of Anyuan Pulverized-Coal Pyrolysis at Different Heating Rates*. Fuel Process. Technol. 148, 295-301.
- ERDOGAN, Y., 2015. *Physicochemical Properties of Handere Clays and Their use as a Building Material*. J. Chem. 1, 1-6.
- FABIO, L.M., FABIO, L., SUSANA, M.S., MONICA, R., PAULO, S.P., CARLOS, R.A., 2009. *Chemical Characterization of Clay SRM by X-Ray Fluorescence Results Comparison from Different Laboratories*. Semina: Cienc. Exatas Tecnol. 30, 2, 145-150.
- FADIL-DJENABOUA, S., NDJIGUIA, P.D., MBEY, J.A., 2015. *Mineralogical and Physicochemical Characterization of Ngaye Alluvial Clays (Northern Cameroon) and Assessment of Its Suitability in Ceramic Production*. J. Asian Ceram. Soc. 3, 50-58.
- GAO, L., RAO, B., DAI, H., XIE, H., WANG, P., MA, F., 2019. *Kinetics of Sulphuric Acid Leaching of Titanium from Refractory Anatase under Atmospheric Pressure*. Physicochem. Probl. Miner. Process. 55, 2, 467-478.
- GARG, N., SKIBSTED, J., 2019. *Dissolution Kinetics of Calcined Kaolinite and Montmorillonite in Alkaline Conditions: Evidence for Reactive Al(V) Sites*. J. Am. Ceram. Soc. 102, 12, 7720-7734.
- GATES, W.P., ANDERSON, J.S., RAVEN, M.D., CHURCHMAN, G.J., 2002. *Mineralogy of a Bentonite from Miles, Queensland, Australia and Characterization of Its Acid Activation Products*. Appl. Clay Sci. 20, 4, 189-197.
- GBOR, P.K., JIA, C.Q., 2004. *Critical Evaluation of Coupling Particle Size Distribution with the Shrinking Core Model*. Chem. Eng. Sci. 59, 1979-1987.
- GHASSA, S., NOAPARAST, M., SHAFAEI, S.Z., ABDOLLAHI, H., GHARABAGHI, M., BORUOMAND, Z., 2017. *A Study on the Zinc Sulfide Dissolution Kinetics with Biological and Chemical Ferric Reagents*. Hydrometallurgy, 171, 362-373.
- HERNANDEZ, R.A., GARCIA, F.L., HERNANDEZ, L.E., LUEVANOS, A.M., 2013. *Iron Removal from Kaolinite Clay by Leaching to Obtain Whiteness Index*. 3rd Congress on Materials Science and Engineering. 1-5.
- HOIDY, W.H., AHMAD, B.A., MULLER, J.A., IBRAHIM, N.A., 2009. *Synthesis and Characterization of Organoclay from Sodium Montmorillonite and Fatty Hydroxamic Acids*. Am. J. Appl. Sci. 6, 8, 1567-1572.
- HURSIT, M., LACIN, O., SARAC, H., 2009. *Dissolution Kinetics of Smithsonite Ore as an Alternative Zinc Source with an Organic Leach Reagent*. J. Taiwan Inst. Chem. Eng. 40, 6-12.
- LEGORRETA, F., SALINAS, E., CERECEDO, E., 2015. *Kinetics Study of Iron Leaching from Kaolinitic Clay Using Oxalic Acid*. Eur. Sci. J. 11, 12, 12-23.
- LEE, O.S., TAM, T., YI, Y.P., SEONG, J.K., MYONG, J.K., 2006. *Study on the Kinetics of Iron Oxide Leaching by Oxalic Acid*. Int. J. Miner. Process. 80, 2, 144-152.
- LI, J., XU, Z., WANG, R., GAO, Y., YANG, Y., 2019. *Study on Leaching Kinetics of Laterite Ore Using Hydrochloric Acid*. Physicochem. Probl. Miner. Process. 55, 3, 711-720.

- LI, M., ZHENG, S., LIU, B., DU, H., DREISINGER, D.B., TAFAGHODI, L., ZHANG, Y., 2017. *The Leaching Kinetics of Cadmium from Hazardous Cu-Cd Zinc Plant Residues*. Waste Manage. 65, 128-138.
- LIMA, P.E.A., ANGÉLICA, R.S., NEVES, R.F., 2017. *Dissolution Kinetics of Amazonian Metakaolin in Hydrochloric Acid*. Clay Miner. 52, 75-82.
- LORI, J.A., LAWAL, A.O., EKANEM, E.J., 2007. *Characterization and Optimization of Deferration of Kankara Clay*. J. Eng. Appl. Sci. 2, 5, 60-74.
- MACCARTHY, J., NOSRATI, A., SKINNER, W., ADDAIMENSAH, J., 2016. *Atmospheric Acid Leaching Mechanisms and Kinetics and Rheological Studies of a Low Grade Saprolitic Nickel Laterite Ore*. Hydrometallurgy. 160, 26-37.
- MADEJOVA, J., BUJDAK, J., JANEK, M., KOMADEL, P., 1998. *Comparative FT-IR Study of Structural Modifications during Acid Treatment of Dioctahedral Smectites and Hectorite*. Spectrochim. Acta, Part A. 54, 1397-1406.
- MANDAL, S.K., BANERJEE, P.C., 2004. *Iron Leaching from China Clay with Oxalic Acid: Effect of Different Physico-Chemical Parameters*. Int. J. Miner. Process. 74, 263-270.
- MILOŠEVIĆ, M., LOGAR, M., KALUĐEROVIĆ, L., JELIĆ, I., 2017. *Characterization of Clays from Slatina (Serbia) for Potential Uses in the Ceramic Industry*. Energy Procedia. 125, 650-655.
- MURRAY, H.H., 1999. *Applied Clay Mineralogy Today and Tomorrow*. Clay Miner. 34, 39-49.
- NAVIAUX, J.D., SUBHAS, A.V., ROLLINS, N.E., DONG, S., BERELSON, W.M., ADKINS, J.F., 2019. *Temperature Dependence of Calcite Dissolution Kinetics in Seawater*. Geochim. Cosmochim. Acta. 246, 363-384.
- NJOKA, E.N., OMBAKA, O., GICHUMBI, J.M., KIBAARA, D.I., NDERI, O.M., 2015. *Characterization of Clays from Tharaka-Nithi County in Kenya for Industrial and Agricultural Applications*. Afr. J. Environ. Sci. Technol. 9, 3, 228-243.
- NZEUKOU, A.N., FAGEL, N., NJOYA, A., KAMGANG, M.V., MEDJO, R.E., MELO, U.C., 2013. *Mineralogy and Physicochemical Properties of Alluvial Clays from Sanaga Valley (Center, Cameroon): Suitability for Ceramic Application*. Appl. Clay Sci. 83, 238-243.
- RAHMAN, M.A., MUNEER, M., 2005. *Photocatalysed Degradation of Two Selected Pesticide Derivatives, Dichloroos and Phosphamidon in Aqueous Suspensions of Titanium Dioxide*. Desalination. 181, 1, 161-172.
- PANIAS, D., TAXIARCHOU, M., DOUNI, I., PASPALIARIS, I., KONTOPOULOS, A., 1996. *Thermodynamic Analysis of the Reactions of Iron Oxides: Dissolution in Oxalic Acid*. Can. Metall. Q. 35, 363-373.
- PARIYAN, K., HOSSEINI, M.R., AHMADI, A., ZAHIRI, A., 2019. *Optimization and Kinetics of Oxalic Acid Treatment of Feldspar for Removing the Iron Oxide Impurities*. Sep. Sci. Technol. 55, 2, 1-12.
- SAIKIA, N.J., BHARALI, D.J., SENGUPTA, P., BORDOLOI, D., GOSWAMEE, R.L., SAIKIA, P.C., BORTHAKUR, P.C., 2003. *Characterization, Beneficiation and Utilization of a Kaolinite Clay from Assam, India*. Appl. Clay Sci. 24, 93-103.
- SAKLAR, S., YORUKOGLU, A., 2015. *Effects of Acid Leaching on Halloysite*. Physicochem. Probl. Miner. Process. 51, 1, 83-94.
- SANDA, O., TAIWO, E.A., 2016. *Investigation of Dissolution Kinetics of a Nigerian Columbite in Hydrofluoric Acid Using the Shrinking Core Model*. Niger. J. Technol. 35, 4, 841-846.
- SANDLER, A., 2013. *Clay Distribution over the Landscape of Israel: from the Hyper-Arid to the Mediterranean Climate Regimes*. Catena. 110, 119-132.
- SANTOS, M.F.M., FUJIWARA, E., SCHENKEL, E.A., ENZWEILER, J., SUZUKI, C.K., 2015. *Processing of Quartz Lumps Rejected by Silicon Industry to Obtain a Raw Material for Silica Glass*. Int. J. Miner. Process. 135, 65-70.
- SEYED-GHASEMI, S.M., AZIZI, A., 2017. *Investigation of Leaching Kinetics of Zinc from a Low-Grade Ore in Organic and Inorganic Acids*. J. Min. Environ. 8, 4, 579-591.
- SHI, Z., BONNEVILLE, S., KROM, M.D., CARSLAW, K.S., JICKELLS, T.D., BAKER, A.R., BENNING, L.G., 2011. *Iron Dissolution Kinetics of Mineral Dust at Low pH During Simulated Atmospheric Processing*. Atmos. Chem. Phys. 11, 995-1007.
- SULTANA, U.K. GULSHAN, F., KURNY, A.S.W., 2014. *Kinetics of Leaching of Iron Oxide in Clay in Oxalic Acid and in Hydrochloric Acid Solutions*. Mater. Sci. Metall. Eng. 2, 1, 5-10.
- SULTANA, U.K., KURNY, A.S.W., 2012. *Dissolution Kinetics of Iron Oxides in Clay in Oxalic Acid Solutions*. Int. J. Miner. Metall. Mater. 19, 1083-1087.
- TANDA, B.C., EKSTEEN, J.J., ORABY, E.A., 2018. *Kinetics of Chalcocite Leaching in Oxygenated Alkaline Glycine Solutions*. Hydrometallurgy. 178, 264-273.
- TAO, L., WANG, L., YANG, K., WANG, X., CHEN, L., NING, P., 2021. *Leaching of Iron from Copper Tailings by Sulfuric Acid: Behavior, Kinetics and Mechanism*. RSC Adv. 11, 5741-5752.

- TEMUJIN, J., JADAMBAA, T., BURMAA, G., ERDENECHIMEG, S., AMARSANAA, J., MACKENZIE, K.J., 2004. *Characterization of Acid Activated Montmorillonite Clay from Tuulant (Mongolia)*. *Ceram. Int.* 30, 251-255.
- TEMUJIN, J., OKADA, K., JADAMBAA, T., MACKENZIE, K.J.D., AMARSANAA, J., 2002. *Effect of Grinding on the Preparation of Porous Material from Talc by Selective Leaching*. *J. Mater. Sci. Lett.* 21, 1607-1609.
- TUNCUK, A., AKCIL, A., 2016. *Iron Removal in Production of Purified Quartz by Hydrometallurgical Process*. *Int. J. Miner. Process.* 153, 1-29.
- VAPUR, H., TOP, S., DEMIRCI, S., 2017. *Purification of Feldspar from Colored Impurities Using Organic Acids*. *Physicochem. Probl. Miner. Process.* 53: 150-160.
- VITRA, R.L., 2009. *U.S. Geological Survey, Mineral Commodity Summaries: Clays*. Washington: United States Government Printing Office, USA.
- WU, M.C., KUO, S.L., LIN, J.C., MA, C.M., HONG, G.B., CHANG, C.T., 2011. *Studies on Certain Physical Properties of Modified Smectite Nanocatalysts*. *Appl. Surf. Sci.* 257, 13, 5641-5646.
- YANG, C.Q., LI, S.Q., 2020. *Kinetics of Iron Removal from Quartz under Ultrasound-Assisted Leaching*. *High Temp. Mater. Process.* 39, 1, 395-404.
- ZHANG, C., MIN, X.B., ZHANG, J.Q., WANG, M., LI, Y.C., FEI, J.C., 2016. *Reductive Clean Leaching Process of Cadmium from Hydrometallurgical Zinc Neutral Leaching Residue Using Sulfur Dioxide*. *J. Clean Prod.* 113, 1, 910-918.
- ZHANG, Q., WEN, S.M., FENG, Q.C., NIE, W.L., WU, D.D., 2017. *Dissolution Kinetics of Hemimorphite in Methane Sulfonic Acid*. *Physicochem. Probl. Miner. Process.* 55, 1, 1-9.
- ZHANG, Q., WEN, S.M., WU, D.D., FENG, Q.C., LI, S., 2019. *Dissolution Kinetics of Hemimorphite in Trichloroacetic Acid Solutions*. *J. Mater. Res. Technol.* 8, 2, 1645-1652.
- ZHONG, L., LEI, S., WANG, E., PEI, Z., LI, L., YANG, Y., 2013. *Research on Removal Impurities from Vein Quartz Sand with Complexing Agents*. *Appl. Mech. Mater.* 454, 194-199.